Dalton Transactions

PERSPECTIVE

View Article Online
View Journal | View Issue

Check for updates

Cite this: *Dalton Trans.*, 2019, **48**, 12365

Low-coordinate first-row transition metal complexes in catalysis and small molecule activation

Laurence J. Taylor and Deborah L. Kays *

Received 6th June 2019,
Accepted 9th July 2019

DOI: 10.1039/c9dt02402f

rsc.li/dalton

Enforcing unusually low coordination numbers on transition metals with sterically demanding ligands has long been an area of interest for chemists. Historically, the synthesis of these challenging molecules has helped to elucidate fundamental principles of bonding and reactivity. More recently, there has been a move towards exploiting these highly reactive complexes to achieve a range of transformations using cheap, earth-abundant metals. In this Perspective, we will highlight selected examples of transition metal complexes with low coordination numbers that have been used in catalysis and the activation of small molecules featuring strong bonds (N_2, CO_2, and CO).

Open Access Article. Published on 29 2019. Downloaded on 2025/11/2 18:52:03.
This article is licensed under a Creative Commons Attribution 3.0 Unported Licence.

Introduction

The stabilisation of transition metal complexes featuring unusually low coordination numbers remains a challenging and active area of research for synthetic inorganic chemists. These species are typically stabilised by sterically demanding ligands, which shield the metal from oligomerisation or further coordination by Lewis basic ligands. To this end, a vast array of bulky ligands have been prepared and utilised for this purpose; including amides,[1] alkyls,[2] silyls,[2] aryls,[3,4] and carbenes.[5,6] The development of such ligands has been instrumental in advancing the range of complexes featuring low-coordinate and highly reactive transition metal centres, and has facilitated the isolation of new classes of compounds,[7] such as species featuring metal–metal multiple bonds.[8]

As the chemistry of low-coordinate complexes has developed, there has been an increasing interest in the exploitation of their reactivity. With the 3d metals, which are cheap and

School of Chemistry, University of Nottingham, University Park, Nottingham, NG7 2RD, UK. E-mail: Deborah.Kays@nottingham.ac.uk

Laurence J. Taylor

Laurence graduated from the University of Cambridge with an MSci in Natural Sciences in 2013. He was then awarded the St Andrews 600th Anniversary Scholarship for his PhD studies at the University of St Andrews under Dr Petr Kilian. After completing his PhD studying air- and moisture-sensitive pnictogen compounds, he took up a post-doctoral position at the University of Nottingham under Professor Deborah Kays in late 2017. His current research focuses on the use of highly reactive complexes of the first-row transition and s-block metals as catalysts for organic transformations.

Deborah L. Kays

Deborah Kays received her MChem and PhD degrees in Chemistry from Cardiff University, Wales. After postdoctoral work, also at Cardiff University, she took up a Junior Research Fellowship at the University of Oxford. She has been at the University of Nottingham since 2007, as Lecturer in Inorganic Chemistry, she was promoted to Associate Professor in 2014 and to Professor in 2019. Her research interests involve the investigation of the stabilisation of highly unsaturated complexes and their reactivity under stoichiometric and catalytic regimes. For her contributions to low-coordinate transition metal chemistry, Deborah was awarded the 2018 RSC Chemistry of the Transition Metals Award.

Open Access Article. Published on 29 2019. Downloaded on 2025/11/2 18:52:03.
This article is licensed under a Creative Commons Attribution 3.0 Unported Licence.

earth-abundant,[9–11] enforcing low-coordinate geometries can drastically alter the reactivity and properties of these elements.[7] For example, two-coordinate 3d metal complexes have been shown to act as single molecule magnets,[12–14] and have been employed in the synthesis of Zintl ions.[15] In recent years, exciting examples of such species catalysing unusual reactions or promoting the activation of challenging substrates have started to appear in the literature. Our research group has become increasingly interested in this field, with some of our recent work looking at the use of *m*-terphenyl complexes in the stoichiometric activation of small molecules and the catalysis of chemical reactions.

The term "low-coordinate" can be a rather tricky one to define when applied to the transition metals. One can argue, for example, that coordination numbers of four could be considered low for high oxidation state iron or vanadium compounds. One could also discuss how to define formal coordination number, and therefore depending on your definition "low-coordinate complexes" could cover a very broad range of species indeed. Given that Perspective articles are meant to be brief, we have restricted ourselves to considering complexes with a formal coordination number of three or less where, for example, ligands such as alkyls, aryls, amides, carbenes, phosphines, alkenes, *etc.* are considered to occupy one coordination site, and η^6-C_6H_6 to occupy three. This is not meant to provide a rigorous definition of "low-coordinate" but has instead been chosen to keep this discussion focused.

Even with this restriction, there are still too many examples for this article to be an exhaustive account of the field. As such, this Perspective will cover selected examples of catalysis and small molecule activation by low-coordinate complexes as defined above.

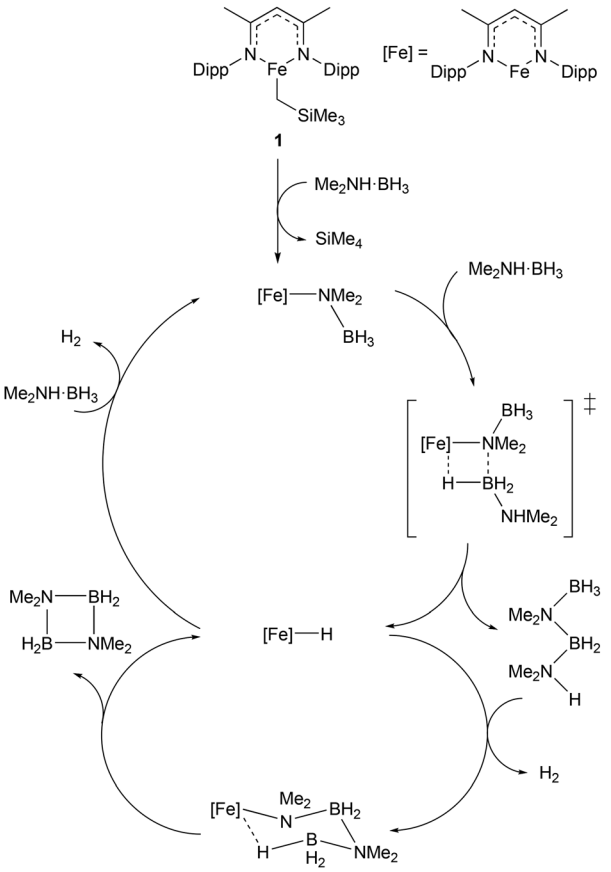

Scheme 1 Example of a three-coordinate iron catalyst with a β-diketiminate ligand (**1**) and the proposed mechanism by which it catalyses the dehydrocoupling of dimethylamine-borane (Dipp = 2,6-*i*Pr$_2$C$_6$H$_3$).[24]

Catalysis

Given the increasing importance of sustainability in catalysis, there has been a shift away from the use of platinum group metals (such as platinum, palladium, and rhodium) towards cheaper and more abundant first-row transition metals.[9–11] In particular, the use of low coordination numbers for 3d transition metal complexes is affording catalysts for a wide range of reactions. A commonly employed ligand system used to support low-coordinate first-row transition metal catalysts is the β-diketiminate; bidentate monoanionic ligands that bind through nitrogen. This ligand has been complexed to numerous metals, and such species have been shown to catalyse a wide variety of transformations including polymerisation,[16,17] catalytic hydrodefluorination,[18,19] *Z*-selective alkene isomerisation,[20] nitrene transfer reactions,[21,22] the dehydrocoupling of phosphines,[23] phosphine-boranes and amine-boranes,[24] and the hydrophosphination[25] and hydroboration[26] of alkenes and alkynes. One example of such a catalyst is shown in Scheme 1, with the three-coordinate iron(II) catalyst (**1**), and the proposed mechanism by which it catalyses the dehydrocoupling of dimethylamine-borane.[24] The development of β-diketiminate 3d complexes as catalysts was covered in a recent Perspective article by Ruth Webster, and we recommend consulting this article for a more in-depth look at such species.[27] Thus, this section will focus on low coordinate 3d metal catalysts that do not feature β-diketiminate ligands. The discussion will be subdivided by metal, to aid clarity.

Nickel

For the most part the metal complexes covered in this review are highly reactive species which have been forced into disfavoured low-coordinate geometries by sterically demanding ligands. However, nickel is something of an exception to this. Complexes of Ni(0) are found to readily adopt two- or three-coordinate geometries when combined with neutral donor ligands such as phosphines and N-heterocyclic carbenes (NHCs), and such species have proven competent catalysts for a broad range of organic transformations. In recent years, there have been examples of C–H activation with the alkenylation,[28] alkylation,[29–31] and stannylation[32] of aromatic systems, C–O bond cleavage,[33–35] and catalytic cycloaddition chemistry.[36] The catalysts are typically generated *in situ* from bis(cyclooctadiene)nickel(0) and the required ligand, with some

 This journal is © The Royal Society of Chemistry 2019

Open Access Article. Published on 29 2019. Downloaded on 2025/11/2 18:52:03.
This article is licensed under a Creative Commons Attribution 3.0 Unported Licence.

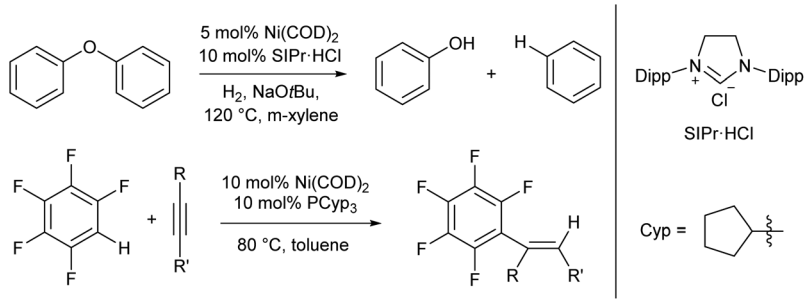

Scheme 2 Hydrogenolysis of aryl ethers[33,34] and alkenylation of arene rings[28] promoted by low coordinate Ni(0) catalysts.

examples from the groups of Hartwig and Nakao shown in Scheme 2.[28,33,34] There are too many examples to cover in detail here, and we recommend that readers interested in the field consult some of the excellent in-depth reviews on this topic.[37,38]

Low-coordinate catalysts based on Ni(I) and Ni(II) are somewhat less common, although certainly not unheard of. For example, several low-coordinate Ni(I) complexes have been investigated as catalysts for Kumada cross-coupling reactions.[12,39–42] The Ni(0) species **2a** and **2b** were reacted with chlorobenzene or bromobenzene to generate the Ni(I) NHC complexes **3a–c** (with elimination of biphenyl),[40,42] all of which catalyse the Kumada reaction (Scheme 3) between aryl magnesium bromides and aryl chlorides or bromides. Compounds **3b–c** also catalysed the coupling of aryl boronic acids to aryl bromides (Suzuki coupling).[42] These complexes are interesting as case studies for the reactivity of low coordinate metals, but more convenient and less sensitive nickel catalysts exist for such transformations.[43]

Matsubara and co-workers found that treatment of **3a** with triphenylphosphine afforded the mixed NHC/phosphine complex **4**, which catalysed the Buchwald–Hartwig amination

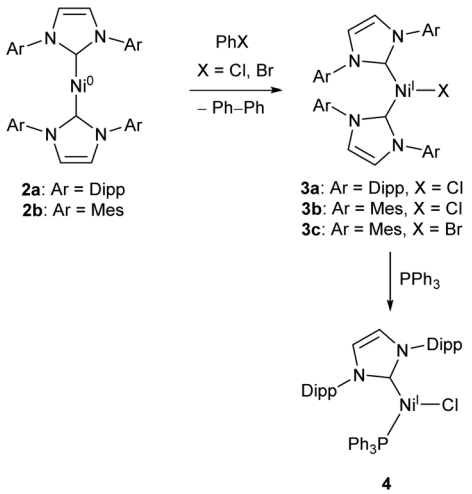

Scheme 3 Synthesis of Ni NHC complexes for Kumada and Suzuki cross-couplings, and Buchwald–Hartwig amination (Dipp = 2,6-iPr$_2$C$_6$H$_3$, Mes = 2,4,6-Me$_3$C$_6$H$_2$).[40–42]

of aryl halides (chlorides, bromides and iodides) by diphenylamine under mild conditions (40–70 °C), affording yields ranging between 41–98% dependent on substrate.[41] The catalyst showed good tolerance of ketone, alkene, and nitro functional groups; providing the first example of a nickel catalyst capable of coupling diphenylamine to aryl halides to afford triphenylamine derivatives (Scheme 3).[41]

Following on from this work, the Matsubara group very recently published an improved Ni(I) amination catalyst (**5a**) which coupled a range of primary and secondary arylamines to 4-bromobenzophenone in yields ranging from 58–96%.[44] The initial pre-catalyst **5a** is four-coordinate, but the active species is believed to be the two-coordinate Ni(I) amide species **5b** (Scheme 4). This species was also synthesised, isolated, and found to be catalytically active.[44] An exchange reaction with 2,2′-biquinoline revealed that the 2,2-bipyridine ligand on **5a** is labile and readily exchanged, allowing for the generation of the active two-coordinate species.[44] EPR spectroscopy of a stoichiometric mixture of **5b** and 4-bromoanisole provided evidence of both Ni(I) and Ni(III) species in solution, providing direct support for the involvement of a Ni(III) intermediate in the catalytic cycle. Such Ni(I)/Ni(III) redox cycles have previously been proposed for a number of nickel catalysts,[45–47] but this study provides some of the best direct evidence for the existence of a Ni(III) intermediate.[44] The catalytic cycle proposed by Matsubara *et al.* is presented in Scheme 4.

Nickel(I) catalysts bearing NHCs of different ring sizes (Scheme 5) were investigated for their efficacy in Kumada cross-coupling reactions, with EPR spectroscopy revealing that the magnetic properties of the complexes were strongly affected by ring size. The NHCs with the smallest ring size gave the best catalysts, although no correlation was observed with the magnetic parameters. The combination of a six-membered ring and mesityl flanking groups was found to give the best catalytic performance, with biaryl yields of 51–83% obtained at room temperature.[12,39]

A two-coordinate Kumada cross-coupling catalyst is seen in the Ni(II) bis(silylamide) complex **6a** reported by Lipschutz and Tilley (Scheme 6).[48–50] This catalyst was more effective for electron-poor aryl halides and, notably, promoted couplings to pyridine-based heterocycles. Stoichiometric reaction of **6a** with MeMgBr resulted in the rapid formation of an alkylated Ni(II) species, **6b**.[48] This compound was found to react over

Open Access Article. Published on 29 2019. Downloaded on 2025/11/2 18:52:03.
This article is licensed under a Creative Commons Attribution 3.0 Unported Licence.

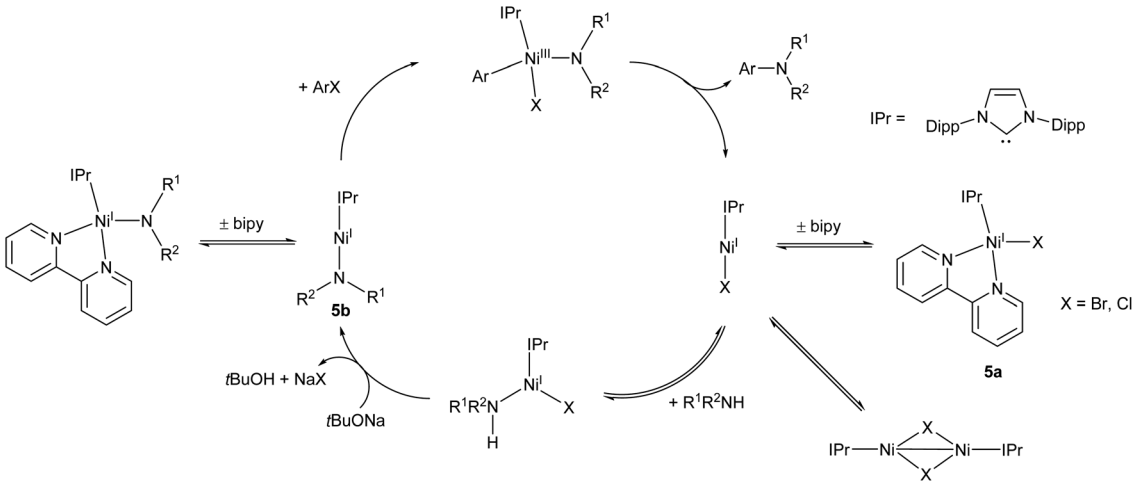

Scheme 4 Proposed mechanism for Buchwald–Hartwig amination by pre-catalyst **5a** proceeding *via* two-coordinate Ni(I) amide **5b**.[44]

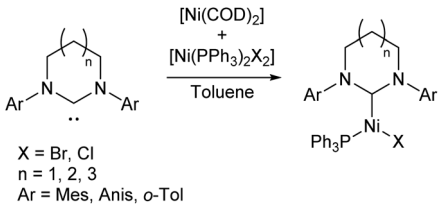

Scheme 5 Synthesis of Ni(I) NHC complexes with varying NHC ring size for Kumada cross-coupling (Anis = 2-$MeOC_6H_4$; *o*-Tol = 2-MeC_6H_4).[12,39]

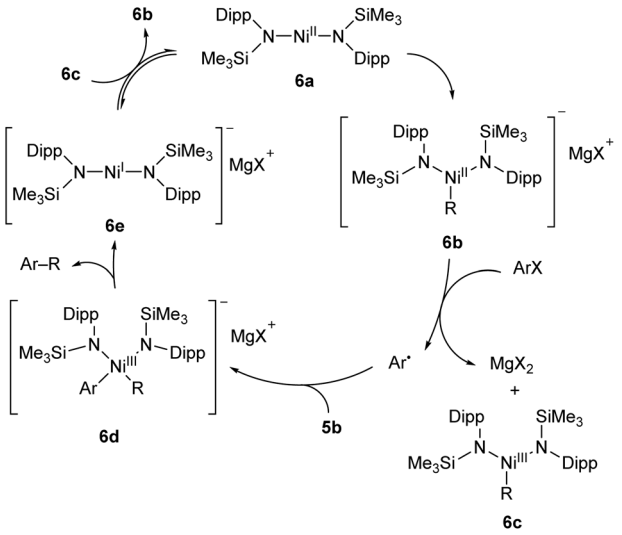

Scheme 6 Proposed reaction mechanism for Kumada cross-coupling catalysed by low-coordinate Ni(II) species **6a**.[48]

45 minutes with 1-iodonaphthalene to afford the coupled product (1-methylnaphthalene) in low yield (13%) along with 1,1′-binaphthalene and Ni(III) methyl complex **6c**. Reacting 1-iodonaphthalene with 2 equivalents of **6b**, by contrast, gave clean and rapid conversion to 1-methylnaphthalene in 98% yield.[48] It is believed that the formation of 1,1′-binaphthalene in the stoichiometric reaction is due to the formation of naphthyl radicals, and the second equivalent of **6b** is required to trap these. The radical nature of this step is supported by a radical clock experiment coupling (iodomethyl)cyclopropane to PhMgBr, which resulted in 4-phenyl-1-butene, the expected product of a radical rearrangement.[48] Finally, an anionic Ni(I) species (**6e**) can be obtained by chemical reduction of **6a**, and the reaction of **6c** and **6e** results in a redox equilibrium affording **6b** and **6a**. Based on the results of these various stoichiometric transformations, Lipschutz and Tilley proposed the catalytic cycle shown in Scheme 6.[48] Species **6a** is also an effective catalyst for the hydrosilylation of 1-octene with diphenylsilane, affording (*n*-octyl)diphenylsilane as the sole product after 2 h at room temperature (5 mol% catalyst loading).[50]

Treatment of the Ni(II) chloride pincer complexes **7a–b** with lithium triethylborohydride affords the four-coordinate Ni(II) hydrides **8a–b**.[51] These complexes can reversibly lose hydrogen, and under ambient pressure exist predominantly as the three coordinate Ni(I) species **9a–b** (Scheme 7a, Fig. 1). The dehydrogenation reaction is second order with respect to **8b**, and likely proceeds *via* a biomolecular elimination reaction.[51] These compounds catalyse hydrodehalogenation reactions, such as the dehalogenation of geminal dihalogenides,[51] and defluorination of geminal difluorocyclopropanes to fluoroalkenes.[52] Such reactions are regarded as a promising route to partially halogenated compounds from readily available perhalogenated species.[53] Both reactions are stereoselective, with moderate ee (enantiomeric excess) values for the monohalides of 20–74%,[51] and high *Z*-selectivity in the formation of alkenes from cyclopropanes.[52] Reactions with (2,2,6,6-tetramethylpiperidin-1-yl)oxyl (TEMPO) resulted in catalyst inhibition, suggesting that the mechanism is radical in nature.[51,52] This was further supported by reactions with radical clock reagents.[51] The proposed catalytic cycle for the dehalogenation of geminal dihalogenides is shown in Scheme 7b.[51]

 This journal is © The Royal Society of Chemistry 2019

Open Access Article. Published on 29 2019. Downloaded on 2025/11/2 18:52:03.
This article is licensed under a Creative Commons Attribution 3.0 Unported Licence.

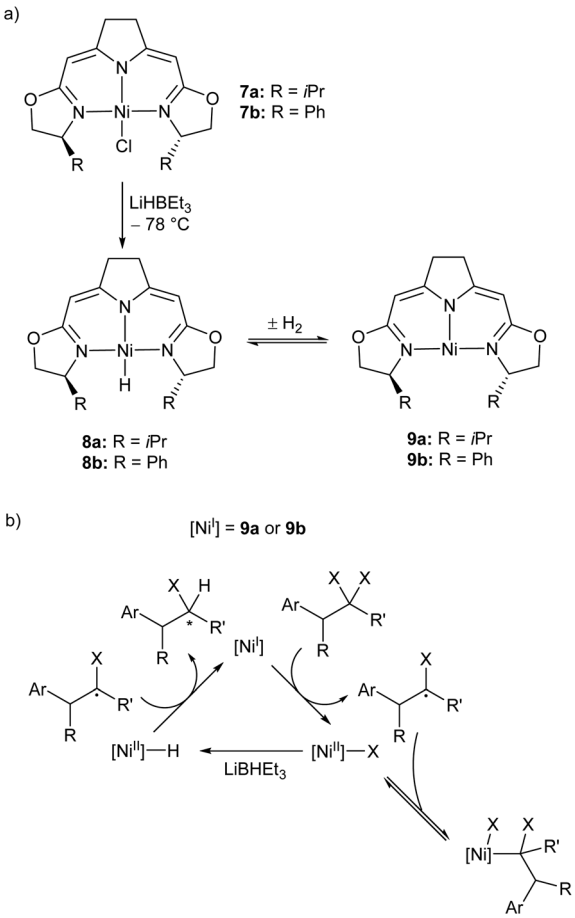

Scheme 7 (a) Synthesis of the three-coordinate Ni(I) species **9a** and **9b**. (b) Proposed mechanism for catalytic, stereoselective hydrodehalogenation of geminal dihalogenides by **9a** and **9b**. $LiBHEt_3$ is used in excess as a reductant and hydride source.[51,52]

The reaction between proligand **10**, *n*BuLi, and *trans*-$[Ni(PPh_3)_2(Ph)Cl]$ resulted in the formation of Ni(I) complex **11**, with concomitant elimination of biphenyl (Scheme 8a).[54] This spontaneous reduction of the nickel centre presumably occurs to reduce the steric demands arising from the bulky bidentate ligand. This three-coordinate species was found to be a remarkably active catalyst for the polymerisation of norbornene in the presence of a methylaluminoxane (MAO) co-catalyst (Scheme 8b), affording high molecular weight polynorbornene (M_w *ca.* 10^6 g mol^{-1}) with catalytic activities of up to 2.82×10^7 g_{PNP} $mol^{-1}{}_{Ni}$ h^{-1}.[54]

Cobalt

Several two- and three-coordinate cobalt catalysts bearing N-heterocyclic carbene (NHC) ligands have been published by Deng and co-workers.[55–59] The three-coordinate Co(I) species **12** was shown to catalyse the hydrosilylation of terminal alkynes, showing broad functional group tolerance and moderate to good selectivity for formation of the *E*-alkene (Scheme 9a).[56] Subsequently, the Co(II) amide species **13**, bearing an asymmetric NHC ligand, catalysed the hydrosilyl-

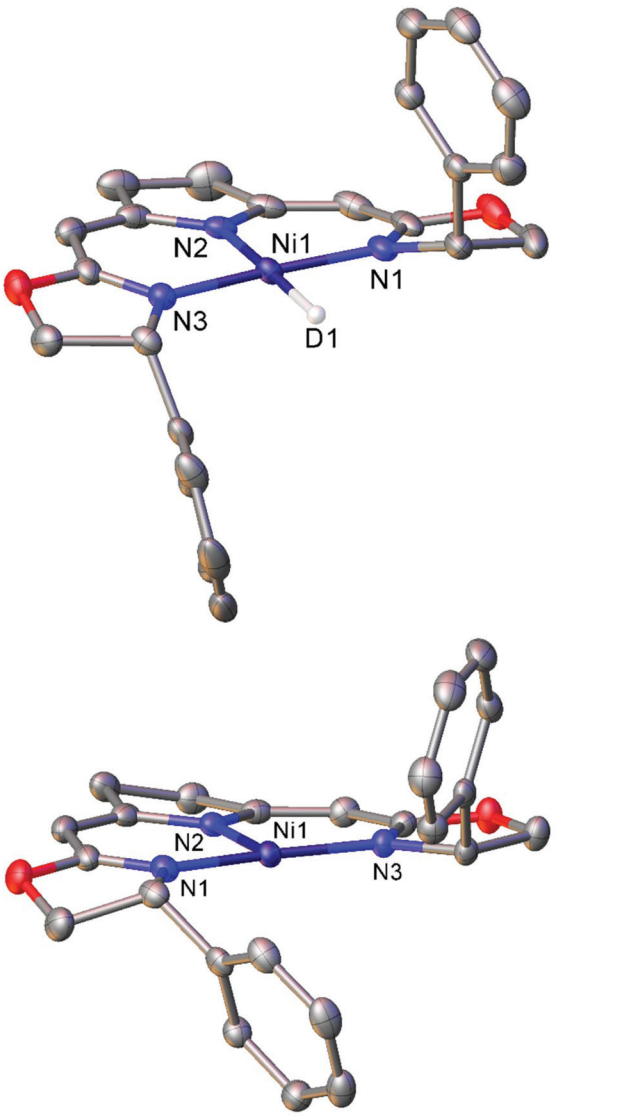

Fig. 1 Molecular structures of the deuterium analogue of **8b** (top) and three-coordinate Ni(I) complex **9b** (bottom). Hydrogen atoms and second molecule in asymmetric unit (**8b**) omitted for clarity. Anisotropic displacement ellipsoids are set at 50% probability.[51]

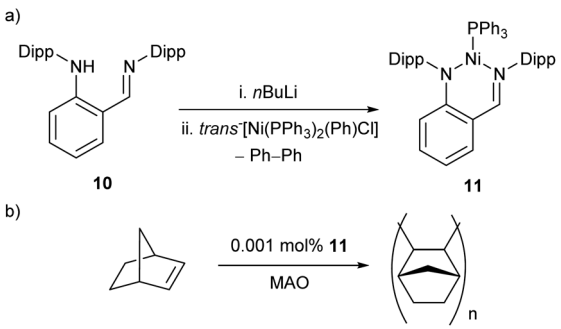

Scheme 8 (a) Synthesis of three-coordinate Ni(I) complex **11** with elimination of biphenyl from a Ni(II) source. (b) Polymerisation of norbornene by **11** in the presence of MAO co-catalyst.[54]

Open Access Article. Published on 29 2019. Downloaded on 2025/11/2 18:52:03.
This article is licensed under a Creative Commons Attribution 3.0 Unported Licence.

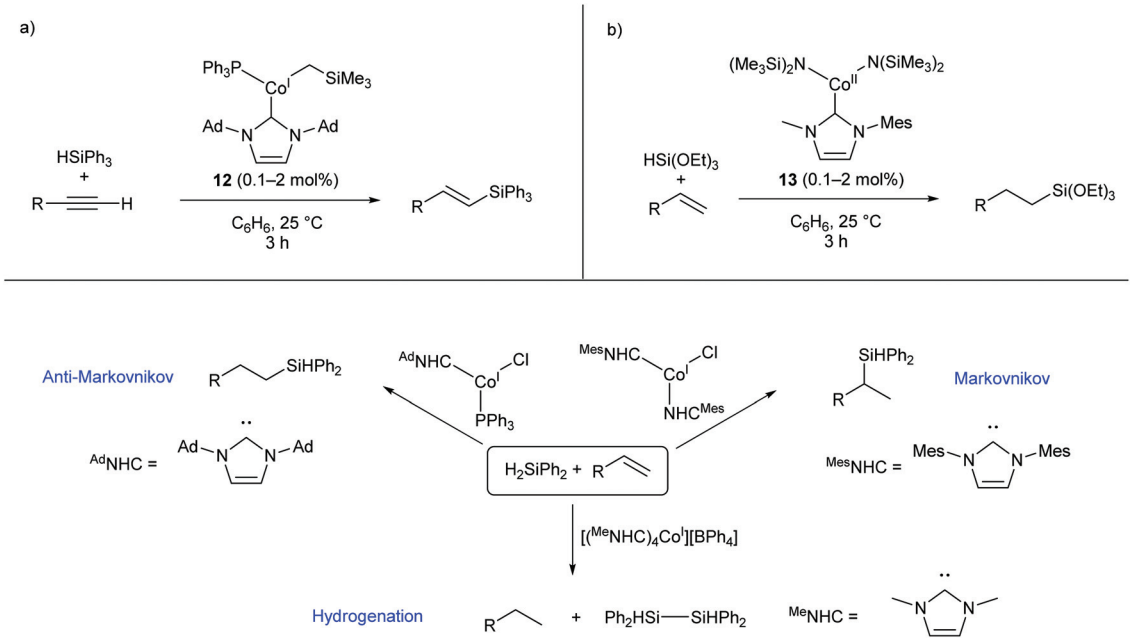

Scheme 9 Cobalt NHC complexes in hydrosilylation reactions. (a) Complex **12**, featuring an NHC and phosphine ligand, selectively gives *E*-alkenes from the reaction of terminal alkynes with triphenylsilane. (b) Co(II) amide NHC complex **13** gives anti-Markovnikov products in the reaction of triethoxysilane with terminal alkenes. (c) Different Co(I) NHC complexes afford different selectivities in the reaction of diphenylsilane with terminal alkenes. Ad = 1-Adamantyl.[55–58]

ation of terminal alkenes affording predominantly anti-Markovnikov products (Scheme 9b).[57] This catalyst was most effective for reactions with triethoxysilane; reactions with other silanes, including triphenylsilane and triethylsilane, gave poor conversions and low yields.[57] Following this investigation, a selection of two-, three-, and four-coordinate Co(I) NHC complexes were able to achieve different selectivity (Markovnikov, anti-Markovnikov, or hydrogenation) for the reaction of diphenylsilane with terminal alkenes, dependent on the choice of catalyst (Scheme 9c).[58] While cobalt hydrosilylation catalysts are widely known, those displaying Markovnikov or hydrogenation selectivity are relatively rare,[58,60,61] so these cobalt NHCs provide a valuable addition to the field.

More recently, the three-coordinate Co(0) complexes **14** and **15** were shown to catalyse the dehydrocoupling of primary arylphosphines to the corresponding diphosphanes (Scheme 10),

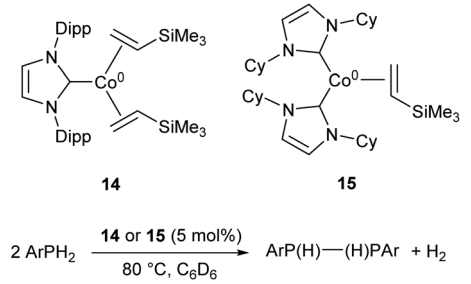

Scheme 10 Dehydrocoupling of primary aryl phosphines by Co(0) NHC complexes **14** and **15**.[59]

an unusual example of a cobalt catalyst for such a transformation.[59] The catalysts afforded the coupled products in moderate to good yields (47–73%), but were ineffective with the secondary phosphine Ph_2PH and primary alkyl phosphine $tBuPH_2$ (7% and 8% yields, respectively).[59]

Manganese and iron

In recent work by our research group, a series of Mn(II) and Fe(II) *m*-terphenyl complexes were found to catalyse the cyclotrimerisation of primary aliphatic isocyanates (Scheme 11).[62] The reactions proceeded cleanly under mild conditions to afford isocyanurates, which find use as polymer additives to improve their physical properties,[63,64] in addition to applications in microporous materials,[65,66] selective ion bonding,[67] and drug delivery.[68–71] Two different flanking aryl groups were employed in the *m*-terphenyl ligands; $[2,6\text{-}Mes_2C_6H_3]^-$, and the less sterically encumbering $[2,6\text{-}Tmp_2C_6H_3]^-$ (Tmp = 2,4,5-$Me_3C_6H_2$), giving catalytically active manganese and iron complexes (**16–19**, Scheme 11a). The Mes-substituted complexes are two-coordinate, while the less bulky Tmp-substituted ligands stabilise three-coordinate complexes, with metal-coordination by an additional THF ligand. While **17** and **19** showed no significant difference in reactivity, two-coordinate **16** was found to give a faster reaction rate than **18**. Catalyst poisoning and radical trap experiments showed no evidence for the formation of catalytic nanoparticles or the involvement of radical processes, and, as a result, the mechanism is postulated to proceed *via* a homogeneous pathway. Kinetic experiments in the reaction of **16** with ethyl isocyanate showed a first order

 This journal is © The Royal Society of Chemistry 2019

Open Access Article. Published on 29 2019. Downloaded on 2025/11/2 18:52:03.
This article is licensed under a Creative Commons Attribution 3.0 Unported Licence.

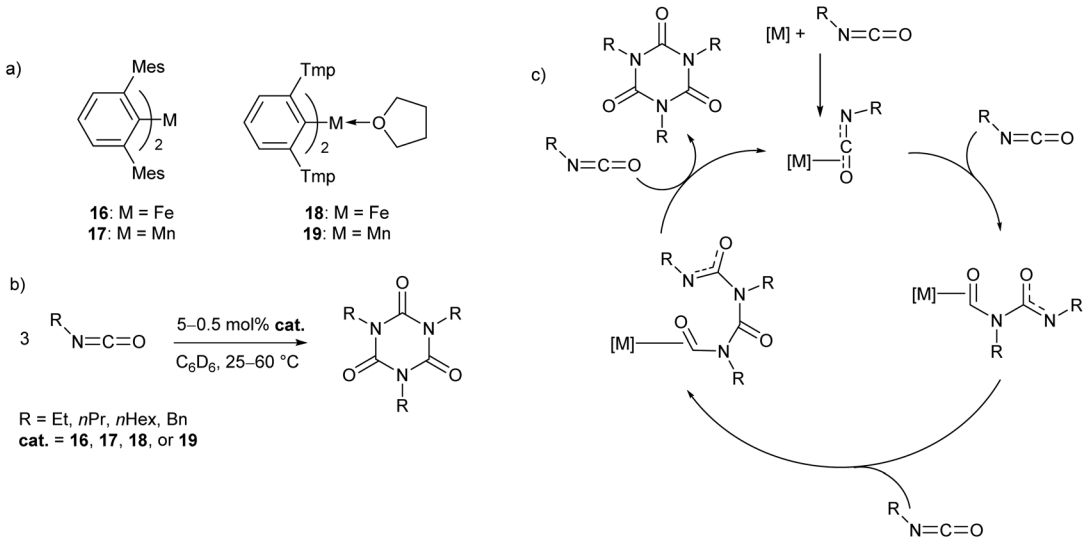

Scheme 11 Cyclotrimerisation of isocyanates with low coordinate *m*-terphenyl metal complexes. (a) Metal complexes used as precatalysts in the cyclotrimerisation reaction. (b) General reaction scheme for cyclotrimerisation of primary aliphatic isocyanates. (c) Proposed Lewis acid mechanism for reaction.[62]

rate dependence in both **16** and substrate. Based on these observations, a mechanism was proposed involving Lewis acid catalysis (Scheme 9c).

The manganese complexes **17**, **19** (Scheme 11a) and the xylyl-substituted analogue catalyse the dehydrocoupling of dimethylamine-borane (Scheme 12),[72] which is of interest in the chemical storage and release of hydrogen.[73–76] While the reaction was slow at room temperature, increasing the reaction temperature to 60 °C provided relatively clean conversion to the cyclic dimer $[Me_2NBH_2]_2$ in high yields and reasonable timeframes. The linear species $Me_2NH–BH_2–NMe_2–BH_3$ was also observed as a side product and intermediate in the reaction. While reactions with the two-coordinate catalyst **17** (and its xylyl analogue) showed no appreciable change upon addition of elemental mercury, reactions with the three-coordinate **19** showed a significant drop in activity. Furthermore, reaction of **19** with $Me_2NH{\cdot}BH_3$ results in the rapid formation of a dark red suspension, while **17** remains a clear yellow solution. This evidence suggests that the reaction with **19** is heterogeneous in nature, involving the formation of catalytic nanoparticles, while reactions with **17** proceed *via* a homogeneous route. This was confirmed by isolation of the manganese nanoparticles from reactions between **19** and $Me_2NH{\cdot}BH_3$, followed by characterisation by transmission electron microscopy (TEM), scanning transmission electron microscopy (STEM) and energy dispersive X-ray spectroscopy (EDX).[72] This reaction serves as an example of how small changes in the steric properties of the flanking aryl groups of *m*-terphenyl ligands can result in significant differences in reactivity.

The iron(II) *m*-terphenyl complexes **16** and **18** (Scheme 11a) are effective catalysts for the hydrophosphination of isocyanates.[77] This reaction affords a mixture of phosphinocarboxamide and phosphinodicarboxamide products, corresponding to both mono- and diinsertion of the isocyanate into the P–H bond (Scheme 13a). Such diinsertion reactions are rare[78] and the double insertion of an isocyanate into a P–H bond has led to a family of phosphinodicarboxamide compounds. By changing the reaction conditions, this reaction can be made selective to afford either the phosphinocarboxamide (reaction in THF solvent) or phosphinodicarboxamide (through the reaction in benzene or toluene solutions in the presence of $Et_3N{\cdot}HCl$) (Scheme 13b).

Reaction monitoring through *in situ* ^1H and ^{31}P NMR spectroscopy reveals that the three-coordinate complex **18** shows significantly higher activity than **16**, which may be due to the presence of a labile THF ligand. Interestingly, reactions with **16** show an induction period of *ca.* 2 h, while no such induction period was observed in reactions catalysed by **18**. Monitoring of stoichiometric reactions by IR spectroscopy suggest that an iron amidate complex may be the active catalytic species in this reaction (Scheme 13c). Poisoning experiments have suggested that the reaction is homogeneous and does not involve radical processes; and a catalytic cycle where the transition metal acts as a Lewis acid was proposed to account for these observations (Scheme 13c).[77]

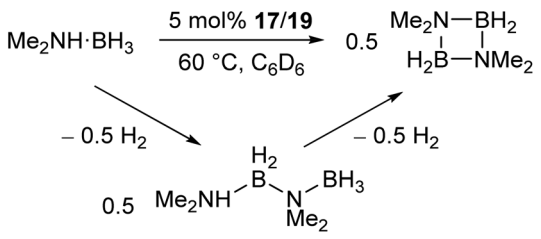

Scheme 12 Dehydrocoupling of $Me_2NH{\cdot}BH_3$ catalysed by low coordinate Mn(II) terphenyl complexes.[72]

Open Access Article. Published on 29 2019. Downloaded on 2025/11/2 18:52:03.
This article is licensed under a Creative Commons Attribution 3.0 Unported Licence.

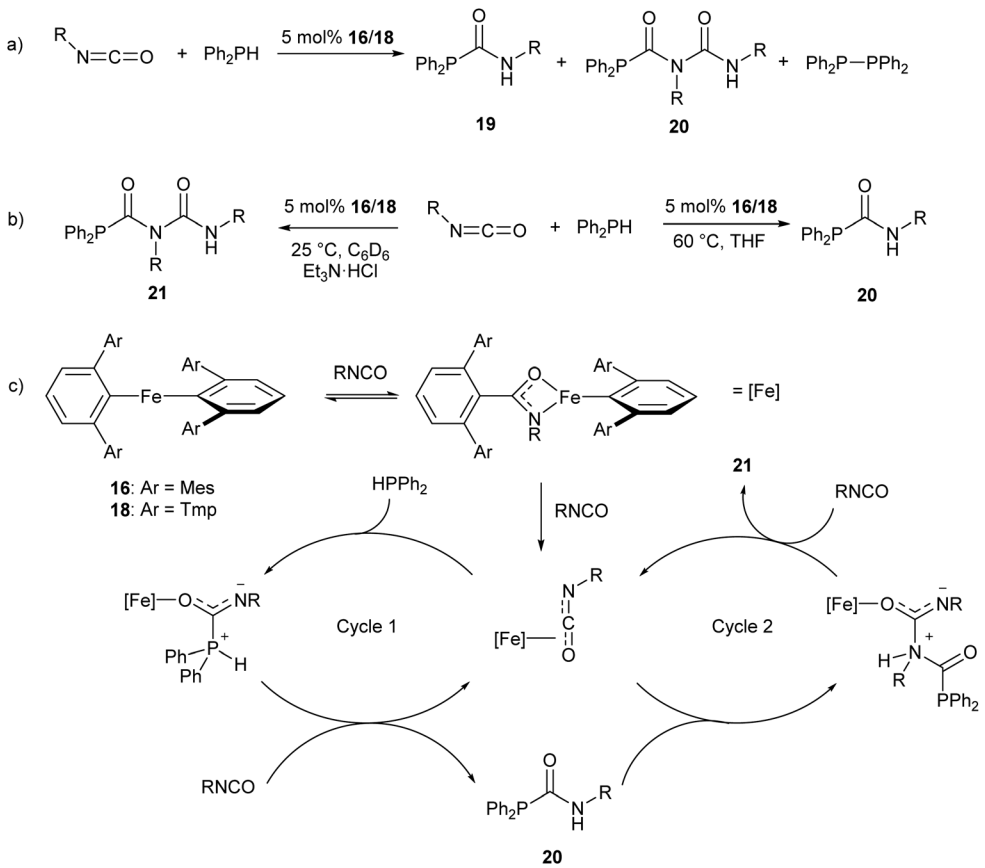

Scheme 13 Iron(II) catalysed hydrophosphination of isocyanates. (a) Initial hydrophosphination conditions affording a mixture of products. R = Ph, *p*-Tol (*p*-Tol = 4-MeC_6H_4), 3,5-$(OMe)_2C_6H_3$, 4-BrC_6H_4, *n*Hex, Cy, *i*Pr, *t*Bu. (b) Optimised conditions for selective formation of monoinsertion (**20**) or diinsertion (**21**) product. (c) Proposed catalytic cycle for formation of observed products.[77]

The two-coordinate Fe(II) amide **22** catalyses the hydrosilylation of ketones, affording the corresponding silyl ethers in good to quantitative yields (Scheme 14b).[79] The catalyst was effective for the reaction of diphenylsilane with a range of ketones, proceeding cleanly at room temperature with low catalyst loadings (0.01–2.7 mol%). However, the reaction failed with tertiary silanes or silanes with bulky substituents, presumably due to steric effects.[79] Species **22** represents an early example of an iron catalyst for this industrially relevant transformation, although it has since been supplanted by more convenient systems.[80]

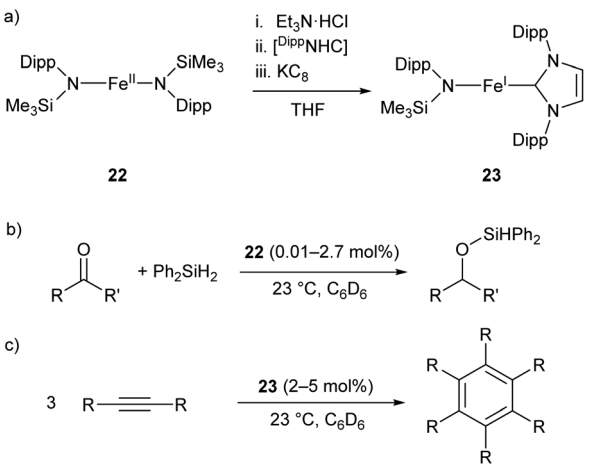

Scheme 14 (a) One-pot synthesis of Fe(I) heteroleptic complex **23** from Fe(II) diamide **22**. [^{Dipp}NHC] = 1,3-bis(2,6-diisopropylphenyl)imidazol-2-ylidene. (b) Hydrosilylation of ketones catalysed by **22**. (c) Cyclotrimerisation of alkynes catalysed by **23**.[79,81]

Complex **22** was later used as the precursor for the (one-pot) synthesis of the first heteroleptic two-coordinate Fe(I) complex **23** (Scheme 14a), which was shown to catalyse the cyclotrimerisation of alkynes to arenes (Scheme 14c).[81] This catalyst was effective at loadings of 2–5 mol% at room temperature, but had limited scope, showing poor reactivity towards substrates with bulky or electron-withdrawing substituents. Nonetheless, the reactivity of this complex is comparable to the handful of iron-based catalysts known for this reaction.[82,83]

Small molecule activation

The activation of small molecules such as N_2, CO_2, and CO poses significant but exciting challenges. Utilising these molecules generally involves overcoming large energy barriers

 This journal is © The Royal Society of Chemistry 2019

Open Access Article. Published on 29 2019. Downloaded on 2025/11/2 18:52:03.
This article is licensed under a Creative Commons Attribution 3.0 Unported Licence.

owing to their high bond strengths and, in some cases, low polarity.[84] However, the activation of such molecules is of significant industrial importance in reactions such as the Haber process and Fischer–Tropsch catalysis.[85] The development of homogeneous systems for functionalising these relatively inert species is thus an area of considerable research interest. In this section, we will outline some examples of low-coordinate first-row transition metal complexes that are able to bind and activate these small molecules.

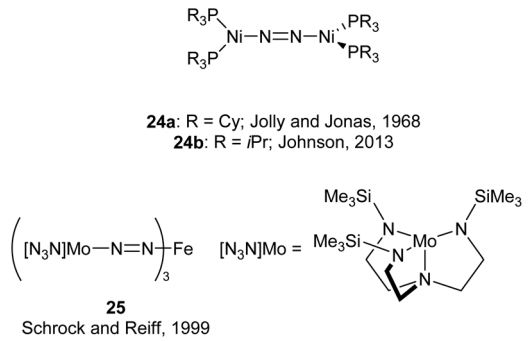

Fig. 2 Notable early examples of 3d metal complexes which bind dinitrogen.

Nitrogen activation

An early example of a low-coordinate 3d metal binding and activating dinitrogen is the nickel phosphine complex **24a**, which was first synthesised in 1968,[86] and crystallographically characterised in 1971 (Fig. 2).[87,88] In this structure, the N_2 unit is protected by a cage of cyclohexyl rings,[87] and a related compound featuring P*i*Pr$_3$ ligands (**24b**) was reported in 2013.[89] Another notable early example of N_2 binding is seen in the mixed Fe/Mo complex **25**, which was the first complex to feature a three-coordinate iron centre coordinated entirely by N_2-derived ligands.[90]

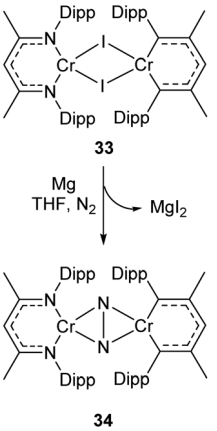

Scheme 16 Synthesis of chromium complex **34**, featuring side-on N_2 coordination.[98]

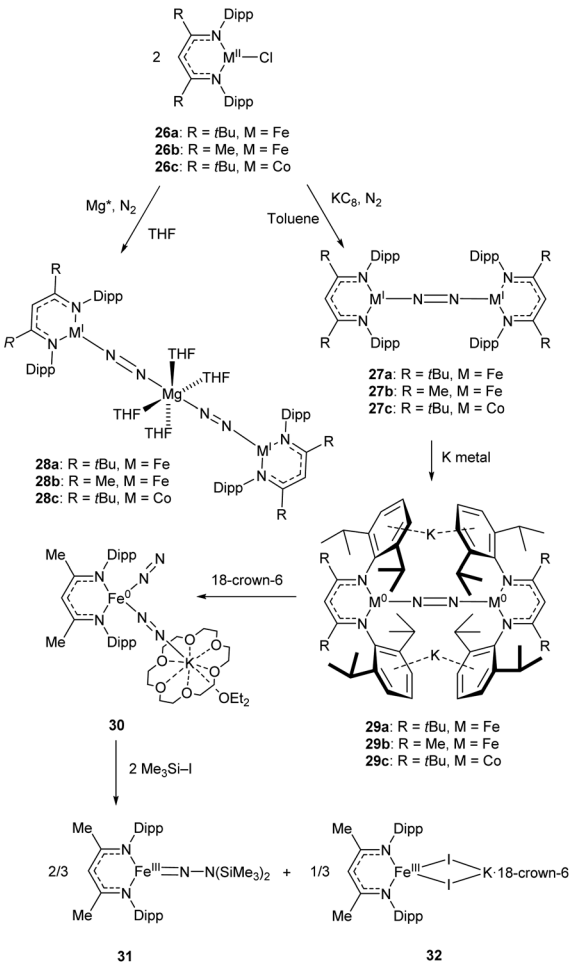

Scheme 15 Synthesis and subsequent reactivity of three-coordinate Fe and Co dinitrogen bridged complexes.[91–97]

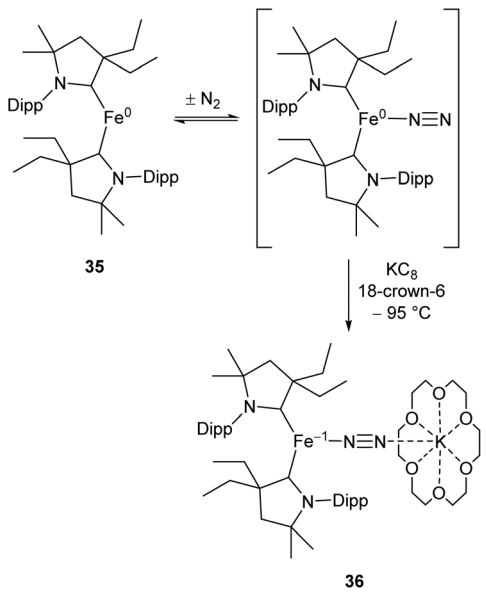

Scheme 17 Reversible binding of N_2 by Fe(CAAC) species **35** and subsequent reduction by KC_8.[102]

Open Access Article. Published on 29 2019. Downloaded on 2025/11/2 18:52:03.
This article is licensed under a Creative Commons Attribution 3.0 Unported Licence.

Some elegant examples of N_2 fixation and activation with low-coordinate 3d metals are seen in the series of iron and cobalt β-diketiminate complexes investigated by the Holland group. Reduction of the metal(II) chloride species (**26a–c**) using KC_8 under a nitrogen atmosphere affords the dinuclear N_2-bridged complexes **27a–c** (Scheme 15).[91–95] Of these N_2-bridged species, complex **27b** was shown to be an effective pre-catalyst for the synthesis of asymmetric carbodiimides from organoazides and isocyanates.[21] The reduction of a THF solution of **26c** with Reike magnesium (Mg*) under a N_2 atmosphere afforded the highly unusual complex **28c**, which features a magnesium bridging between two N_2 ligands.[96] This complex was sufficiently stable for isolation and characterisation by single crystal X-ray diffraction. The corresponding Mg* reductions with **26a** and **26b** afforded the metastable Fe complexes **28a** and **28b**, which could only be characterised in THF solution by infrared (ν_{NN} = 1808 cm^{-1} for **28a**; 1818 cm^{-1} for **28b**) and Mössbauer spectroscopy.

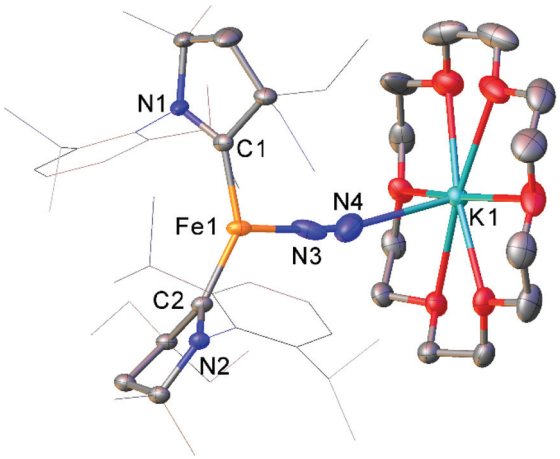

Fig. 3 Molecular structure of **36**. Hydrogen atoms omitted and flanking groups of CAAC ligands are depicted as wireframe for clarity. Anisotropic displacement ellipsoids are set at 50% probability.[102]

Complexes **27a–c** can also be reduced by potassium to afford the metal(0) species **29a–c**, which features two K^+ ions coordinated to the aromatic Dipp rings.[91–95] The side-on coordination of K^+ results in elongated N=N bonds [**29a** 1.233(6) Å; **29b** 1.215(6) Å; **29c** 1.220(2) Å],[91–95] compared to those observed in **27a–c** [**27a** 1.189(4) Å; **27b** 1.186(7) Å; **27c** 1.139(2) Å].[91–95] Treatment of the reduced iron species **29b** with 18-crown-6 affords a new four-coordinate complex **30**, in which potassium is coordinated by an N_2 ligand.[97] This species is active towards silylation, reacting with Me_3SiI to afford the three-coordinate Fe(III) hydrazido species **31** along with Fe(II) iodide **32**.[97] It should be noted that reacting **29b** with Me_3SiI directly affords **31** in low yields (*ca.* 5%) with long reaction times.

Complexes **27a–c** can be compared with the closely related chromium complex **34**, prepared by Theopold and co-workers.[98] Despite having a very similar ligand framework, in **34** the two nickel atoms bind dinitrogen side-on rather than end on as in **27a–c**. Complex **34** was prepared by magnesium reduction of the Cr(II) iodide **33** in THF solution under a nitrogen atmosphere (Scheme 16). This side-on coordination results in greater lengthening of the N–N bond (1.249(5) Å in **34**)[98] compared with the end-on coordination of **27a–c**.

While the binding and partial reduction of dinitrogen in this manner presents exciting possibilities, the full reduction of nitrogen to ammonia by a homogeneous catalyst remains a challenging prospect.[99,100] One example of a low-coordinate complex which is capable of reducing N_2 in this manner is the Fe cyclic alkyl amino carbene (CAAC) complex **35**, recently published by Peters, Ung and co-workers.[101,102] This two-coordinate complex was capable of binding N_2 reversibly at low temperatures (*ca.* −78 °C) which resulted in significant changes in the UV/Vis spectra of a solution in pentane.[102] The reaction between this complex and KC_8 at −95 °C in the presence of

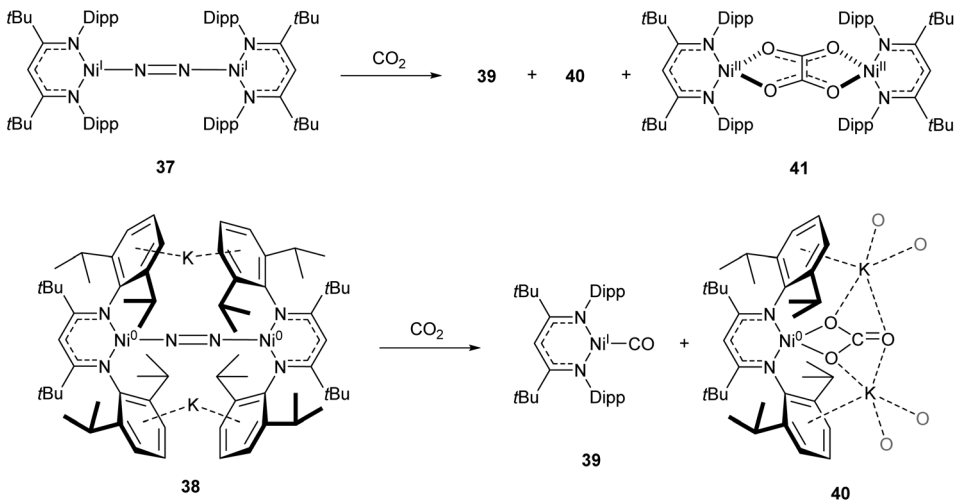

Scheme 18 CO_2 fixation and activation by dinitrogen-bridged nickel complexes **37** and **38**.[109–111]

 This journal is © The Royal Society of Chemistry 2019

Open Access Article. Published on 29 2019. Downloaded on 2025/11/2 18:52:03.
This article is licensed under a Creative Commons Attribution 3.0 Unported Licence.

18-crown-6 facilitated the isolation of the Fe(−I) complex **36** (Scheme 17), the structure of which was confirmed by X-ray crystallography (Fig. 3). Attempting this reaction at temperatures above −78 °C resulted in decomposition to a complex mixture of products. The treatment of **35** with an excess of both KC_8 and $HBAr^F_4{\cdot}OEt_2$ ($[BAr^F_4]^-$ = tetrakis(3,5-bis(trifluoromethyl)phenyl)borate) at −95 °C in diethyl ether under a dinitrogen atmosphere allowed for the catalytic generation of ammonia, albeit with modest turnover numbers (3.3 ± 1.1 equivalents of NH_3 per Fe). Reactions at temperatures above −95 °C were ineffective, which is attributed to the poor binding of N_2 to **35** at elevated temperatures.[102]

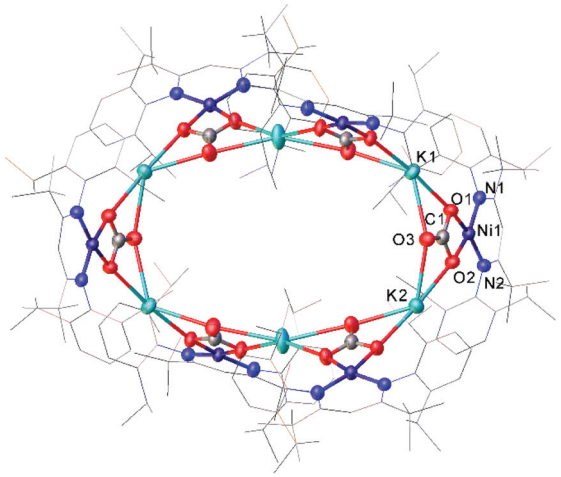

Fig. 4 Molecular structure of **40**. Hydrogen atoms and co-crystallised hexane omitted and carbon atoms of β-diketiminate ligands are depicted as wireframe for clarity. Anisotropic displacement ellipsoids are set at 50% probability.[112]

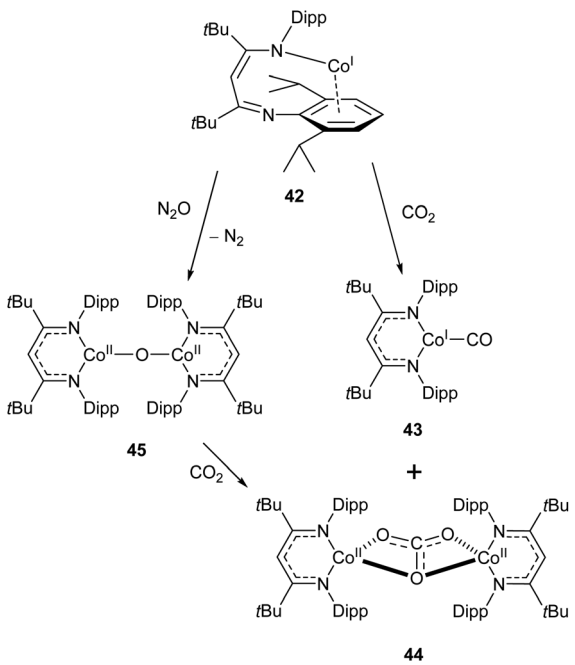

Scheme 19 Reactivity of "slipped" Co(I) β-diketiminate complex **42** with CO_2 and N_2O.[114,115]

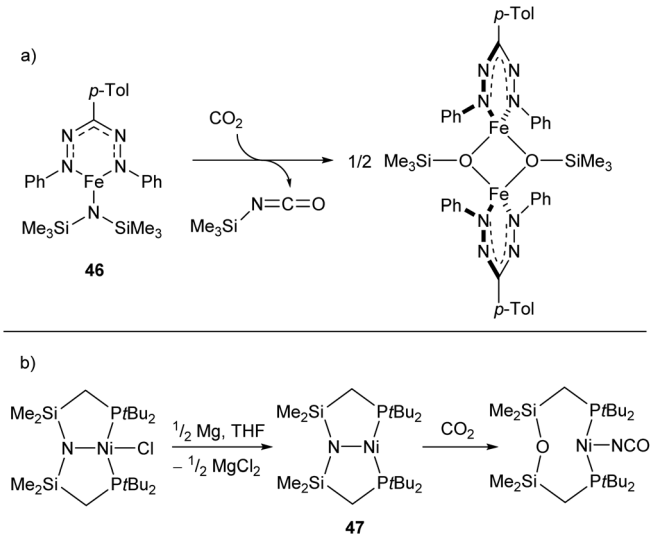

Scheme 20 (a) Formation of isocyanate from reaction of CO_2 with iron-silylamide complex **46**. (b) Transposition reaction of Ni complex **47** with CO_2 to generate Ni(I) isocyanate.[124,125]

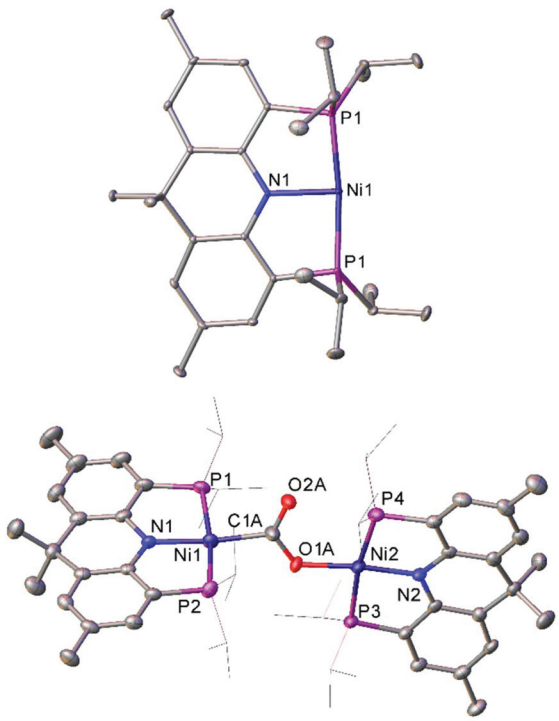

Fig. 5 Molecular structure of T-shaped Ni(I) complex **48** (top), and the species obtained after treating with CO_2 (**49**, bottom). Hydrogen atoms, co-crystallised naphthalene (**48**) and disorder in carboxylate group (**49**) omitted, and *i*Pr groups (**49**) are depicted as wireframe for clarity. Anisotropic displacement ellipsoids are set at 50% probability.[127]

Open Access Article. Published on 29 2019. Downloaded on 2025/11/2 18:52:03.
This article is licensed under a Creative Commons Attribution 3.0 Unported Licence.

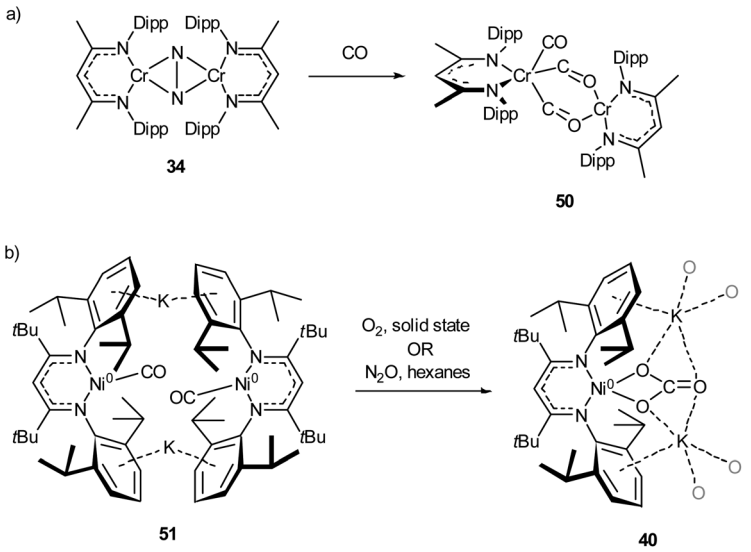

Scheme 21 (a) Reaction of chromium dinitrogen complex **34** with CO to give bridged isocarbonyl complex **50**.[98] (b) Oxidation of CO to carbonate by reaction with O_2 or N_2O with **51**.[112]

Carbon dioxide activation

One common example of carbon dioxide activation by low-coordinate 3d metals is the co-polymerisation of CO_2 and epoxides by Zn β-diketiminate complexes, with a significant number of reports on this subject.[103–108] The reaction is postulated to be an example of Lewis acid catalysis, and recent work has shown that introducing electron withdrawing CF_3 groups into the ligand framework can drastically increase turnover frequency for these catalysts.[106–108]

A Ni complex (**37**), closely related to the Fe and Co complexes **27a–c** shown in Scheme 15, was synthesised by Limberg and co-workers by reduction of the corresponding nickel(II) bromide with potassium triethylborohydride under a nitrogen atmosphere.[109] This complex can be further reduced to the Ni(0) species **38** by reaction with KC_8. Both complexes were able to activate carbon dioxide, undergoing reductive coupling and cleavage to generate Ni(I)CO (**39**), Ni(II)CO_3 (**40**), and Ni(II)C_2O_4Ni(II) (**41**) species (Scheme 18).[110,111] Complex **40** forms a macrocyclic structure in the solid state, consisting of six nickel and six potassium cations, which was characterised by X-ray diffraction (Fig. 4). All of the Ni(II) centres in this structure are square planar and possess low spin configurations. Complex **40** was also synthesised by reacting a Ni(0)CO complex with either N_2O or O_2, a highly unusual example of CO oxidation at nickel.[112] The iron dinitrogen complex **27a** (Scheme 15) reacted with CO_2 in a similar manner, affording the first four-coordinate iron dicarbonyl complex, and a carbonate-bridged diiron complex.[113]

Similar reactivity towards CO_2 was demonstrated by the Co(I) β-diketiminate complex **42**, which features a highly unusual slipped κN,η^6-arene coordination mode.[114,115] The reaction between this compound and CO_2 affords the monocarbonyl complex **43** and dicobalt carbonate complex **44** (Scheme 19). The mechanism has been probed by DFT calculations, and is considered to proceed *via* the oxo-bridged dimer **45**, which was synthesised independently by reaction of **43** with N_2O. The reaction between **45** and CO_2 afforded **44** as the sole product (Scheme 19).[115]

Reactions between low-coordinate metal amides and carbon dioxide can afford isocyanates, carbodiimides, or (often) a mixture of the two. While the reaction has been performed with metals from the s-,[116,117] p-,[118–120] and f-block,[121,122] zinc- and iron-based systems have shown some of the greatest selectivities,[123,124] with a recent iron silylamide (**46**) affording the corresponding isocyanate with >95% selectivity at CO_2 pressures as low as 0.01 atm (Scheme 20a).[124] A related reaction is seen with the PNP-pincer Ni(I) complex **47**,[125] which undergoes a transposition of the ligand N atom on reaction with CO_2 to afford a POP-pincer and Ni(I) isocyanate (Scheme 18b).[126]

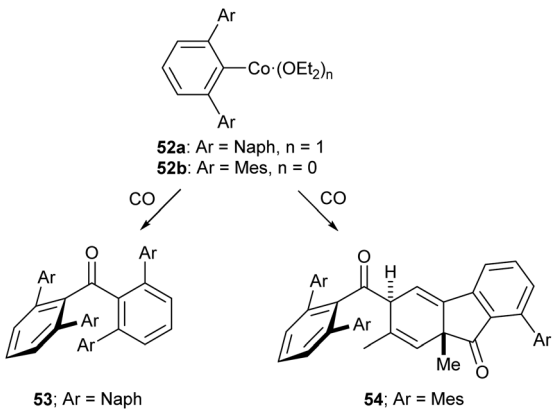

Scheme 22 Reactions of Co *m*-terphenyl complexes with CO to afford sterically encumbered ketones. Naph = 1-Naphthyl, 1-$C_{10}H_7$.[131]

 This journal is © The Royal Society of Chemistry 2019

Open Access Article. Published on 29 2019. Downloaded on 2025/11/2 18:52:03.
This article is licensed under a Creative Commons Attribution 3.0 Unported Licence.

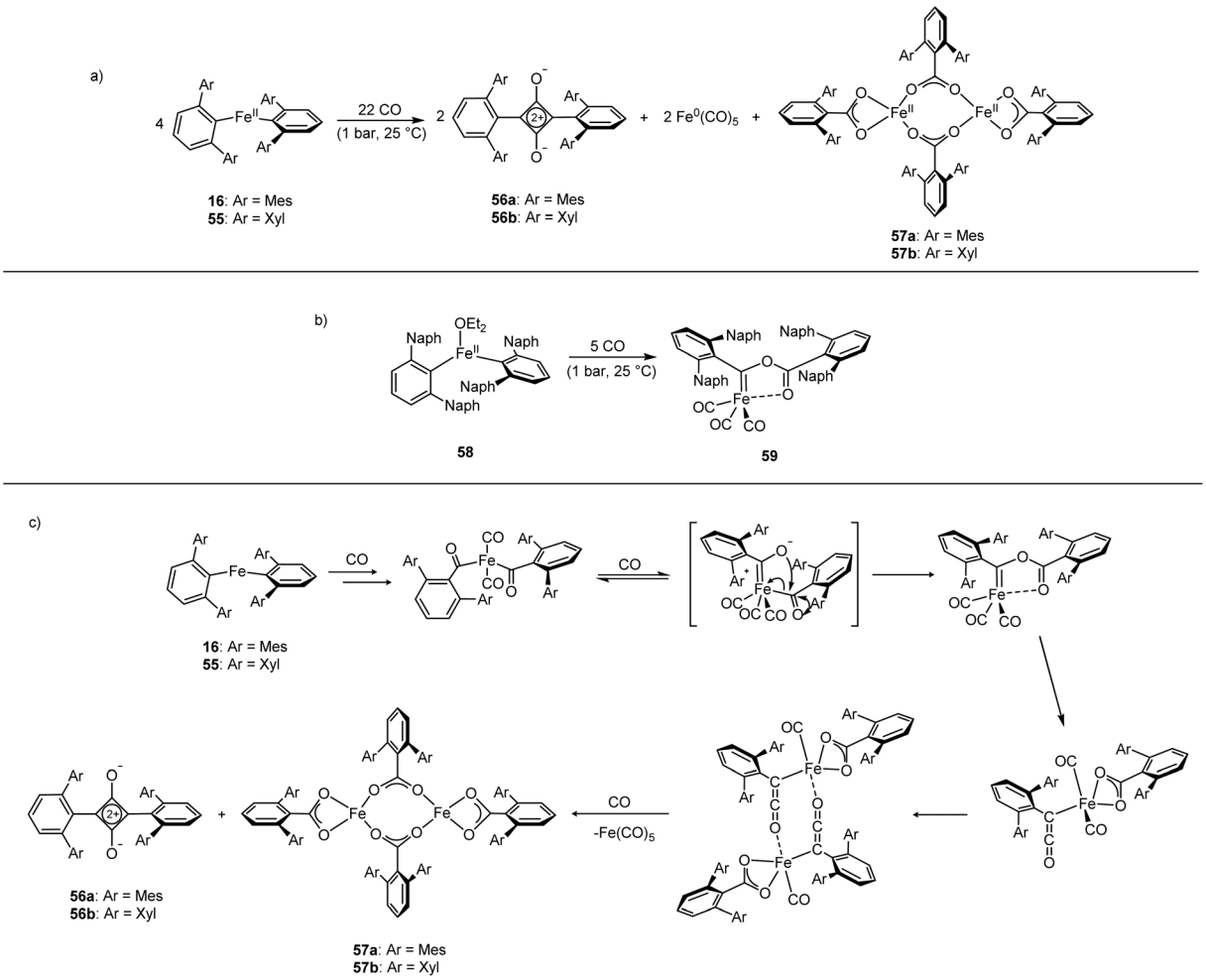

Scheme 23 Reactions of Fe(II) *m*-terphenyl complexes with CO. (a) Mes and Xyl substituted compounds (**16** and **55**) react to give squaraines (**56a–b**), iron carboxylates (**57a–b**), and $Fe(CO)_5$. (b) Naphthyl substituted **58** reacts with CO to afford iron-carbene **59**. (c) Proposed mechanism for the reaction between **16** or **55** with CO.[132]

The T-shaped Ni(I) complex **48**, which features a rigid acridane-based ligand, was recently investigated by Yoo and Lee.[127] This species was obtained by reduction of the corresponding Ni(II) chloride by sodium naphthalenide, and proved capable of activating a diverse range of small molecules under mild conditions. Notably, **48** reduced carbon dioxide under ambient conditions, affording the carboxylate-bridged species **49** (Fig. 5). The complex can also reduce ethene to an ethane bridge, and causes homolytic bond cleavage of a range of molecules; including dihydrogen, methanol, phenol, diphenyl disulfide, methyl iodide, hydrazine, and acetonitrile.[127]

Reactivity towards carbon monoxide

The activation of carbon monoxide by low-coordinate 3d species is less explored than that of CO_2 or N_2, with the majority of low-coordinate complexes simply binding CO to give the corresponding metal carbonyls.[89,92,125,127] Examples of more interesting reactivity include the chromium dinitrogen complex **34**, which reacts with CO to afford the bridged complex **50**,[98] a relatively rare example of an isocarbonyl complex.[128] Compound **50** features activated CO molecules bridging through both the carbon and oxygen atoms with a diamagnetic mixed valent Cr(II)/Cr(0) core (Scheme 21a).[98] The three-coordinate Ni(0) carbonyl complex **51** (Scheme 21b) is capable of oxidising CO in the presence of N_2O or O_2 to give the macrocyclic carbonate complex **40**,[112] previously seen in Scheme 18 and Fig. 4 as the result of CO_2 activation.[110]

Of the low-coordinate 3d complexes investigated for CO activation, *m*-terphenyl complexes have arguably shown the most promise. There are examples of such complexes undergoing CO insertion reactions to afford carbonyl complexes, such as metal acyl species.[129,130] The cobalt(II) complexes **52a** and **52b** reacted with CO to afford sterically encumbered ketones.[131] These reactions proceeded cleanly at room temperature affording either a benzophenone (**53**) or a keto-fluorenone (**54**) depending on the flanking aryl group (Scheme 22).[131]

The Fe(II) complexes **16** and **55** reduce CO with complete scission of the C≡O bond, affording the highly unusual squar-

Open Access Article. Published on 29 2019. Downloaded on 2025/11/2 18:52:03.
This article is licensed under a Creative Commons Attribution 3.0 Unported Licence.

aines **56a–b**, with concomitant formation of the Fe(II) carboxylate complexes **57a–b** and $Fe(CO)_5$ (Scheme 23a, Fig. 6).[132] This reaction proceeds cleanly at room temperature and 1 bar pressure, and is both the first example of reductive cleavage of CO by a low-coordinate iron complex[133,134] and C_4 ring formation from CO with complete C≡O bond cleavage.[135] The squaraines **56a–b** feature broken conjugation due to the steric bulk of the aryl substituents, which forces them out-of-plane with the C_4O_2 ring. This results in less delocalisation into the aromatic rings, giving an unusually high C=O IR stretching frequency (**56a** = 1673 cm^{-1}) and carbonyl chemical shift (**56a** δ_c = 269.7 ppm) in comparison to other squaraines.[136–139] Reactions with ^{13}CO proved that all four carbon atoms in the central squaraine ring are derived from CO, and monitoring by IR spectroscopy has suggested that ketene or ketenyl (C=C=O) intermediates may be formed during the reaction. The analogous reaction using the related *m*-terphenyl complex **58**, which features flanking 1-naphthyl substituents, has facilitated the isolation of Fe(II) carbene **59** (Scheme 23b), which is postulated to be an intermediate in the formation of squaraines from **16** and **55**. It is proposed that the reaction halts at **59** due to the increased steric demands of the flanking naphthyl groups, which prevent further reaction. Indeed, naphthyl-substituted *m*-terphenyl complexes are known to display conformational isomerism due to restricted rotation,[140] and the results of DFT calculations support the notion that these flanking groups halt the reaction at species **59**. Based upon these observations, a mechanism was proposed that accounts for the formation of these products, and fits all the available mechanistic data (Scheme 23c).[132]

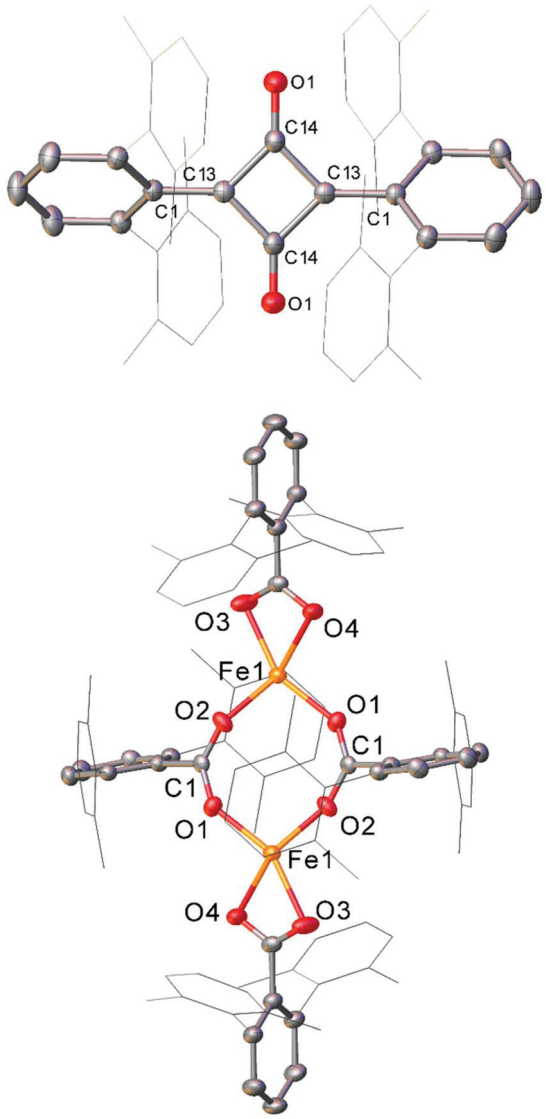

Fig. 6 Molecular structure of sterically encumbered squaraine **56b** (top), and iron carboxylate **57b** (bottom). Hydrogen atoms omitted and flanking xylyl groups depicted as wireframe for clarity. Anisotropic displacement ellipsoids are set at 50% probability.[132]

Conclusions and outlook

Although the use of low-coordinate, first-row metal complexes in catalysis and small molecule activation is a relatively young field, this strategy shows considerable promise for achieving reactivity that would be challenging by other means. Already, a vast array of diverse and exciting transformations has been discovered, and we feel confident that this research area will continue to grow and develop in the future. One thing we noted while composing this perspective is the relatively narrow range of 3d metals that dominate this area. Cobalt, nickel and iron are by far the most thoroughly investigated elements, with manganese, chromium and copper[141] appearing less frequently, for example. It is possible that the less-explored elements could yield as-yet unseen reactivity, and we hope to see more work in this area in the future.

It is highly likely that the preparation of new bulky ligands with different electronic properties will be key to the development of future low-coordinate catalysts and reagents. Of particular interest are the relatively new class of cyclic (alkyl)(amino)carbenes (CAACs), which are more σ-donating and π-accepting than N-heterocyclic carbenes;[142] and the recently developed $[2,6\text{-}(2,4,6\text{-}t\mathrm{Bu}_3\mathrm{C}_6\mathrm{H}_2)_2\mathrm{C}_6\mathrm{H}_3]^-$, an incredibly sterically encumbering *m*-terphenyl ligand,[143] which was recently exploited in the synthesis of several Sn–Sn bonded compounds.[144]

Finally, we note the increasing interest in mechanistic investigations of these catalysts, with more researchers undertaking kinetic measurements of these systems rather than simply viewing the reaction as a "black box". Hopefully this will lead to a greater understanding of the factors that underpin the reactivity of low-coordinate metal species and allow for the future rational design of improved catalytic systems.

Conflicts of interest

There are no conflicts to declare.

This journal is © The Royal Society of Chemistry 2019

Open Access Article. Published on 29 2019. Downloaded on 2025/11/2 18:52:03.
This article is licensed under a Creative Commons Attribution 3.0 Unported Licence.

Acknowledgements

We gratefully acknowledge the Engineering and Physical Sciences Research Council [grant number EP/R004064/1] and the University of Nottingham for their support.

References

1 D. L. Kays, *Chem. Soc. Rev.*, 2016, **45**, 1004–1018.
2 P. P. Power, *J. Organomet. Chem.*, 2004, **689**, 3904–3919.
3 D. L. Kays, *Dalton Trans.*, 2011, **40**, 769–778.
4 D. L. Kays, in *Organometallic Chemistry*, 2010, vol. 36, pp. 56–76.
5 L. Falivene, A. Poater and L. Cavallo, in *N-Heterocyclic Carbenes: Effective Tools for Organometallic Synthesis*, ed. S. P. Nolan, Wiley-VCH, 1st edn., 2014, pp. 25–38.
6 A. Schmidt, S. Wiechmann and C. F. Otto, in *Advances in Heterocyclic Chemistry*, ed. E. F. V. Scriven and C. A. Ramsden, Elsevier Ltd, 2016, vol. 119, pp. 143–172.
7 P. P. Power, *Chem. Rev.*, 2012, **112**, 3482–3507.
8 T. Nguyen, A. D. Sutton, M. Brynda, J. C. Fettinger, G. J. Long and P. P. Power, *Science*, 2005, **310**, 844–847.
9 P. Chirik and R. Morris, *Acc. Chem. Res.*, 2015, **48**, 2495–2495.
10 L. L. Schafer, P. Mountford and W. E. Piers, *Dalton Trans.*, 2015, **44**, 12027–12028.
11 S. Enthaler, K. Junge and M. Beller, *Angew. Chem., Int. Ed.*, 2008, **47**, 3317–3321.
12 M. J. Page, W. Y. Lu, R. C. Poulten, E. Carter, A. G. Algarra, B. M. Kariuki, S. A. MacGregor, M. F. Mahon, K. J. Cavell, D. M. Murphy and M. K. Whittlesey, *Chem. – Eur. J.*, 2013, **19**, 2158–2167.
13 J. M. Zadrozny, D. J. Xiao, M. Atanasov, G. J. Long, F. Grandjean, F. Neese and J. R. Long, *Nat. Chem.*, 2013, **5**, 577–581.
14 Y. S. Meng, Z. Mo, B.-W. Wang, Y.-Q. Zhang, L. Deng and S. Gao, *Chem. Sci.*, 2015, **6**, 7156–7162.
15 B. Zhou, M. S. Denning, D. L. Kays and J. M. Goicoechea, *J. Am. Chem. Soc.*, 2009, **131**, 2802–2803.
16 V. C. Gibson, E. L. Marshall, D. Navarro-Llobet, A. J. P. White and D. J. Williams, *J. Chem. Soc., Dalton Trans.*, 2002, 4321–4322.
17 M.-S. Zhou, S.-P. Huang, L.-H. Weng, W.-H. Sun and D.-S. Liu, *J. Organomet. Chem.*, 2003, **665**, 237–245.
18 J. Vela, J. M. Smith, Y. Yu, N. A. Ketterer, C. J. Flaschenriem, R. J. Lachicotte and P. L. Holland, *J. Am. Chem. Soc.*, 2005, **127**, 7857–7870.
19 N. M. Hein, F. S. Pick and M. D. Fryzuk, *Inorg. Chem.*, 2017, **56**, 14513–14523.
20 C. Chen, T. R. Dugan, W. W. Brennessel, D. J. Weix and P. L. Holland, *J. Am. Chem. Soc.*, 2014, **136**, 945–955.
21 R. E. Cowley, M. R. Golder, N. A. Eckert, M. H. Al-Afyouni and P. L. Holland, *Organometallics*, 2013, **32**, 5289–5298.
22 S. Wiese, M. J. B. Aguila, E. Kogut and T. H. Warren, *Organometallics*, 2013, **32**, 2300–2308.
23 A. K. King, A. Buchard, M. F. Mahon and R. L. Webster, *Chem. – Eur. J.*, 2015, **21**, 15960–15963.
24 N. T. Coles, M. F. Mahon and R. L. Webster, *Organometallics*, 2017, **36**, 2262–2268.
25 M. Espinal-Viguri, A. K. King, J. P. Lowe, M. F. Mahon and R. L. Webster, *ACS Catal.*, 2016, **6**, 7892–7897.
26 M. Espinal-Viguri, C. R. Woof and R. L. Webster, *Chem. – Eur. J.*, 2016, **22**, 11605–11608.
27 R. L. Webster, *Dalton Trans.*, 2017, **46**, 4483–4498.
28 Y. Nakao, N. Kashihara, K. S. Kanyiva and T. Hiyama, *J. Am. Chem. Soc.*, 2008, 16170–16171.
29 J. S. Bair, Y. Schramm, A. G. Sergeev, E. Clot, O. Eisenstein and J. F. Hartwig, *J. Am. Chem. Soc.*, 2014, **136**, 13098–13101.
30 S. Okumura, S. Tang, T. Saito, K. Semba, S. Sakaki and Y. Nakao, *J. Am. Chem. Soc.*, 2016, **138**, 14699–14704.
31 Y. Schramm, M. Takeuchi, K. Semba, Y. Nakao and J. F. Hartwig, *J. Am. Chem. Soc.*, 2015, **137**, 12215–12218.
32 S. A. Johnson, *Dalton Trans.*, 2015, **44**, 10905–10913.
33 N. I. Saper and J. F. Hartwig, *J. Am. Chem. Soc.*, 2017, **139**, 17667–17676.
34 A. G. Sergeev and J. F. Hartwig, *Science*, 2011, **332**, 439–443.
35 J. Cornella, E. Gómez-Bengoa and R. Martin, *J. Am. Chem. Soc.*, 2013, **135**, 1997–2009.
36 A. Thakur and J. Louie, *Acc. Chem. Res.*, 2015, **48**, 2354–2365.
37 B. M. Rosen, K. W. Quasdorf, D. A. Wilson, N. Zhang, A.-M. Resmerita, N. K. Garg and V. Percec, *Chem. Rev.*, 2011, **111**, 1346–1416.
38 N. A. Harry, S. Saranya, S. M. Ujwaldev and G. Anilkumar, *Catal. Sci. Technol.*, 2019, **9**, 1726–1743.
39 E. Carter and D. M. Murphy, *Top. Catal.*, 2015, **58**, 759–768.
40 S. Miyazaki, Y. Koga, T. Matsumoto and K. Matsubara, *Chem. Commun.*, 2010, **46**, 1932–1934.
41 S. Nagao, T. Matsumoto, Y. Koga and K. Matsubara, *Chem. Lett.*, 2011, **40**, 1036–1038.
42 K. Zhang, M. Conda-Sheridan, S. R. Cooke and J. Louie, *Organometallics*, 2011, **30**, 2546–2552.
43 S. Z. Tasker, E. A. Standley and T. F. Jamison, *Nature*, 2014, **509**, 299–309.
44 T. Inatomi, Y. Fukahori, Y. Yamada, R. Ishikawa, S. Kanegawa, Y. Koga and K. Matsubara, *Catal. Sci. Technol.*, 2019, **9**, 1784–1793.
45 L. Iffland, A. Petuker, M. van Gastel and U.-P. Apfel, *Inorganics*, 2017, **5**, 78.
46 I. Kalvet, Q. Guo, G. J. Tizzard and F. Schoenebeck, *ACS Catal.*, 2017, **7**, 2126–2132.
47 X. Lin and D. L. Phillips, *J. Org. Chem.*, 2008, **73**, 3680–3688.
48 M. I. Lipschutz and T. D. Tilley, *Angew. Chem., Int. Ed.*, 2014, **53**, 7290–7294.
49 A. N. Vedernikov, *ChemCatChem*, 2014, **6**, 2490–2492.
50 M. I. Lipschutz and T. D. Tilley, *Chem. Commun.*, 2012, **48**, 7146–7148.

Open Access Article. Published on 29 2019. Downloaded on 2025/11/2 18:52:03.
This article is licensed under a Creative Commons Attribution 3.0 Unported Licence.

51 C. Rettenmeier, H. Wadepohl and L. H. Gade, *Chem. – Eur. J.*, 2014, **20**, 9657–9665.
52 J. Wenz, C. A. Rettenmeier, H. Wadepohl and L. H. Gade, *Chem. Commun.*, 2016, **52**, 202–205.
53 M. F. Kuehnel, D. Lentz and T. Braun, *Angew. Chem., Int. Ed.*, 2013, **52**, 3328–3348.
54 H.-Y. Wang, X. Meng and G. Jin, *Dalton Trans.*, 2006, 2579–2585.
55 J. Sun and L. Deng, *ACS Catal.*, 2016, **6**, 290–300.
56 Z. Mo, J. Xiao, Y. Gao and L. Deng, *J. Am. Chem. Soc.*, 2014, **136**, 17414–17417.
57 Y. Liu and L. Deng, *J. Am. Chem. Soc.*, 2017, **139**, 1798–1801.
58 Y. Gao, L. Wang and L. Deng, *ACS Catal.*, 2018, **8**, 9637–9646.
59 D. Wang, Q. Chen, X. Leng and L. Deng, *Inorg. Chem.*, 2018, **57**, 15600–15609.
60 B. Raya, S. Jing, V. Balasanthiran and T. V. RajanBabu, *ACS Catal.*, 2017, **7**, 2275–2283.
61 B. Raya, S. Biswas and T. V. Rajanbabu, *ACS Catal.*, 2016, **6**, 6318–6323.
62 H. R. Sharpe, A. M. Geer, H. E. L. Williams, T. J. Blundell, W. Lewis, A. J. Blake and D. L. Kays, *Chem. Commun.*, 2017, **53**, 937–940.
63 J. M. Kenny, L. Torre and L. M. Chiacchiarelli, *J. Appl. Polym. Sci.*, 2015, **132**, 42750.
64 G. Wegener, M. Brandt, L. Duda, J. Hofmann, B. Klesczewski, D. Koch, R. Kumpf, H. Orzesek, H.-G. Pirkl, C. Six, C. Steinlein and M. Weisbeck, *Appl. Catal., A*, 2001, **221**, 303–335.
65 Y. Zhang, S. N. Riduan and J. Y. Ying, *Chem. – Eur. J.*, 2009, **15**, 1077–1081.
66 E. Preis, N. Schindler, S. Adrian and U. Scherf, *ACS Macro Lett.*, 2015, **4**, 1268–1272.
67 M. Mascal, I. Yakovlev, E. B. Nikitin and J. C. Fettinger, *Angew. Chem., Int. Ed.*, 2007, **46**, 8782–8784.
68 P. Gibbons, D. Love, T. Craig and C. Budke, *Vet. Parasitol.*, 2016, **218**, 1–4.
69 A. Bosco, L. Rinaldi, G. Cappelli, A. Saratsis, L. Nisoli and G. Cringoli, *Vet. Parasitol.*, 2015, **212**, 408–410.
70 A. P. Murray and M. J. Miller, *J. Org. Chem.*, 2003, **68**, 191–194.
71 M. Ghosh and M. J. Miller, *J. Org. Chem.*, 1994, **59**, 1020–1026.
72 H. R. Sharpe, A. M. Geer, T. J. Blundell, F. R. Hastings, M. W. Fay, G. A. Rance, W. Lewis, A. J. Blake and D. L. Kays, *Catal. Sci. Technol.*, 2018, **8**, 229–235.
73 S. Bhunya, T. Malakar, G. Ganguly and A. Paul, *ACS Catal.*, 2016, **6**, 7907–7934.
74 E. M. Leitao, T. Jurca and I. Manners, *Nat. Chem.*, 2013, **5**, 817–829.
75 A. Staubitz, A. P. M. Robertson and I. Manners, *Chem. Rev.*, 2010, **110**, 4079–4124.
76 A. Staubitz, A. P. M. Robertson, M. E. Sloan and I. Manners, *Chem. Rev.*, 2010, **110**, 4023–4078.
77 H. R. Sharpe, A. M. Geer, W. Lewis, A. J. Blake and D. L. Kays, *Angew. Chem., Int. Ed.*, 2017, **56**, 4845–4848.
78 Y. Sun, Z. Zhang, X. Wang, X. Li, L. Weng and X. Zhou, *Dalton Trans.*, 2010, **39**, 221–226.
79 J. Yang and T. D. Tilley, *Angew. Chem., Int. Ed.*, 2010, **49**, 10186–10188.
80 B. A. F. Le Bailly and S. P. Thomas, *RSC Adv.*, 2011, **1**, 1435–1445.
81 M. I. Lipschutz, T. Chantarojsiri, Y. Dong and T. D. Tilley, *J. Am. Chem. Soc.*, 2015, **137**, 6366–6372.
82 A. Casitas, H. Krause, R. Goddard and A. Fürstner, *Angew. Chem., Int. Ed.*, 2015, **54**, 1521–1526.
83 B. A. Frazier, V. A. Williams, P. T. Wolczanski, S. C. Bart, K. Meyer, T. R. Cundari and E. B. Lobkovsky, *Inorg. Chem.*, 2013, **52**, 3295–3312.
84 W. B. Tolman, *Activation of Small Molecules: Organometallic and Bioinorganic Perspectives*, Wiley, 1st edn, 2006.
85 J. Hagen, *Industrial Catalysis: A Practical Approach*, Wiley, 3rd edn, 2015.
86 P. W. Jolly and K. Jonas, *Angew. Chem.*, 1968, **80**, 705.
87 P. W. Jolly, K. Jonas, C. Krüger and Y.-H. Tsay, *J. Organomet. Chem.*, 1971, **33**, 109–122.
88 This initial complex was followed by some other interesting nickel N_2 complexes by the same authors; see: (*a*) K. Jonas, *Angew. Chem., Int. Ed. Engl.*, 1973, **12**, 997–998; (*b*) C. Kruger and Y.-H. Tsay, *Angew. Chem., Int. Ed. Engl.*, 1973, **12**, 998–999; (*c*) K. Jonas, D. J. Brauer, C. Kruger, P. J. Roberts and Y.-H. Tsay, *J. Am. Chem. Soc.*, 1976, **98**, 74–81.
89 R. Beck, M. Shoshani, J. Krasinkiewicz, J. A. Hatnean and S. A. Johnson, *Dalton Trans.*, 2013, **42**, 1461–1475.
90 M. B. O'Donoghue, W. M. Davis, R. R. Schrock and W. M. Reiff, *Inorg. Chem.*, 1999, **38**, 243–252.
91 J. M. Smith, R. J. Lachicotte, K. A. Pittard, T. R. Cundari, G. Lukat-Rodgers, K. R. Rodgers and P. L. Holland, *J. Am. Chem. Soc.*, 2001, **123**, 9222–9223.
92 J. M. Smith, A. R. Sadique, T. R. Cundari, K. R. Rodgers, G. Lukat-Rodgers, R. J. Lachicotte, C. J. Flaschenriem, J. Vela and P. L. Holland, *J. Am. Chem. Soc.*, 2006, **128**, 756–769.
93 S. F. McWilliams and P. L. Holland, *Acc. Chem. Res.*, 2015, **48**, 2059–2065.
94 P. L. Holland, *Acc. Chem. Res.*, 2008, **41**, 905–914.
95 K. Ding, A. W. Pierpont, W. W. Brennessel, G. Lukat-Rodgers, K. R. Rodgers, T. R. Cundari, E. Bill and P. L. Holland, *J. Am. Chem. Soc.*, 2009, **131**, 9471–9472.
96 T. R. Dugan, K. C. MacLeod, W. W. Brennessel and P. L. Holland, *Eur. J. Inorg. Chem.*, 2013, 3891–3897.
97 S. F. McWilliams, E. Bill, G. Lukat-Rodgers, K. R. Rodgers, B. Q. Mercado and P. L. Holland, *J. Am. Chem. Soc.*, 2018, **140**, 8586–8598.
98 W. H. Monillas, G. P. A. Yap, L. A. Macadams and K. H. Theopold, *J. Am. Chem. Soc.*, 2007, **129**, 8090–8091.
99 K. C. MacLeod and P. L. Holland, *Nat. Chem.*, 2013, **5**, 559–565.

 This journal is © The Royal Society of Chemistry 2019

Open Access Article. Published on 29 2019. Downloaded on 2025/11/2 18:52:03.
This article is licensed under a Creative Commons Attribution 3.0 Unported Licence.

100 Y. Roux, C. Duboc and M. Gennari, *ChemPhysChem*, 2017, **18**, 2606–2617.
101 G. Ung, J. Rittle, M. Soleilhavoup, G. Bertrand and J. C. Peters, *Angew. Chem., Int. Ed.*, 2014, **53**, 8427–8431.
102 G. Ung and J. C. Peters, *Angew. Chem., Int. Ed.*, 2015, **54**, 532–535.
103 M. Cheng, E. B. Lobkovsky and G. W. Coates, *J. Am. Chem. Soc.*, 1998, **120**, 11018–11019.
104 D. R. Moore, M. Cheng, E. B. Lobkovsky and G. W. Coates, *J. Am. Chem. Soc.*, 2003, **125**, 11911–11924.
105 C. M. Byrne, S. D. Allen, E. B. Lobkovsky and G. W. Coates, *J. Am. Chem. Soc.*, 2004, **126**, 11404–11405.
106 S. Kissling, M. W. Lehenmeier, P. T. Altenbuchner, A. Kronast, M. Reiter, P. Deglmann, U. B. Seemann and B. Rieger, *Chem. Commun.*, 2015, **51**, 4579–4582.
107 M. Reiter, A. Kronast, S. Kissling and B. Rieger, *ACS Macro Lett.*, 2016, **5**, 419–423.
108 M. Reiter, S. Vagin, A. Kronast, C. Jandl and B. Rieger, *Chem. Sci.*, 2017, **8**, 1876–1882.
109 S. Pfirrmann, C. Limberg, C. Herwig, R. Stößer and B. Ziemer, *Angew. Chem., Int. Ed.*, 2009, **48**, 3357–3361.
110 B. Horn, C. Limberg, C. Herwig and B. Braun, *Chem. Commun.*, 2013, **49**, 10923–10925.
111 P. Zimmermann and C. Limberg, *J. Am. Chem. Soc.*, 2017, **139**, 4233–4242.
112 B. Horn, C. Limberg, C. Herwig, M. Feist and S. Mebs, *Chem. Commun.*, 2012, **48**, 8243–8245.
113 A. R. Sadique, W. W. Brennessel and P. L. Holland, *Inorg. Chem.*, 2008, **47**, 784–786.
114 T. R. Dugan, X. Sun, E. V. Rybak-Akimova, O. Olatunji-Ojo, T. R. Cundari and P. L. Holland, *J. Am. Chem. Soc.*, 2011, **133**, 12418–12421.
115 L. Roy, M. H. Al-Afyouni, D. E. DeRosha, B. Mondal, I. M. DiMucci, K. M. Lancaster, J. Shearer, E. Bill, W. W. Brennessel, F. Neese, S. Ye and P. L. Holland, *Chem. Sci.*, 2019, **10**, 918–929.
116 V. U. Wannagat, H. Kuckertz, C. Krüger and J. Pump, *Z. Anorg. Allg. Chem.*, 1964, **333**, 54–61.
117 D. A. Dickie, K. B. Gislason and R. A. Kemp, *Inorg. Chem.*, 2012, **51**, 1162–1169.
118 L. R. Sita, J. R. Babcock and R. Xi, *J. Am. Chem. Soc.*, 1996, **118**, 10912–10913.
119 J. R. Babcock and L. R. Sita, *J. Am. Chem. Soc.*, 1998, **120**, 5585–5586.
120 C. A. Stewart, D. A. Dickie, B. Moasser and R. A. Kemp, *Polyhedron*, 2012, **32**, 14–23.
121 H. Yin, P. J. Carroll and E. J. Schelter, *Chem. Commun.*, 2016, **52**, 9813–9816.
122 C. Camp, L. Chatelain, C. E. Kefalidis, J. Pécaut, L. Maron and M. Mazzanti, *Chem. Commun.*, 2015, **51**, 15454–15457.
123 A. M. Felix, B. J. Boro, D. A. Dickie, Y. Tang, J. A. Saria, B. Moasser, C. A. Stewart, B. J. Frost and R. A. Kemp, *Main Group Chem.*, 2012, **11**, 13–29.
124 D. L. J. Broere, B. Q. Mercado and P. L. Holland, *Angew. Chem., Int. Ed.*, 2018, **57**, 6507–6511.
125 M. J. Ingleson, B. C. Fullmer, D. T. Buschhorn, H. Fan, M. Pink, J. C. Huffman and K. G. Caulton, *Inorg. Chem.*, 2008, **47**, 407–409.
126 B. C. Fullmer, H. Fan, M. Pink and K. G. Caulton, *Inorg. Chem.*, 2008, **47**, 1865–1867.
127 C. Yoo and Y. Lee, *Angew. Chem., Int. Ed.*, 2017, **56**, 9502–9506.
128 *Isocarbonyl Complexes in Encyclopedia of Inorganic Chemistry*, ed. R. B. King, R. H. Crabtree, C. M. Lukehart, D. A. Atwood and R. A. Scott, 2006.
129 H. Lei, B. D. Ellis, C. Ni, F. Grandjean, G. J. Long and P. P. Power, *Inorg. Chem.*, 2008, **47**, 10205–10207.
130 C. Ni and P. P. Power, *Chem. Commun.*, 2009, 5543–5545.
131 B. M. Gridley, A. J. Blake, A. L. Davis, W. Lewis, G. J. Moxey and D. L. Kays, *Chem. Commun.*, 2012, **48**, 8910–8912.
132 H. R. Sharpe, A. M. Geer, L. J. Taylor, B. M. Gridley, T. J. Blundell, A. J. Blake, E. S. Davies, W. Lewis, J. McMaster, D. Robinson and D. L. Kays, *Nat. Commun.*, 2018, **9**, 3757.
133 Z. Mo and L. Deng, *Coord. Chem. Rev.*, 2017, **350**, 285–299.
134 D. Benito-Garagorri, I. Lagoja, L. F. Veiros and K. A. Kirchner, *Dalton Trans.*, 2011, **40**, 4778–4792.
135 It should be noted that the formation of squarates $(C_4O_4)^{2-}$ from CO is known, but this does not require the cleavage of C≡O bonds. See: N. Tsoureas, O. T. Summerscales, F. G. N. Cloke and S. M. Roe, *Organometallics*, 2013, **32**, 1353–1362.
136 G. Xia and H. Wang, *J. Photochem. Photobiol., C*, 2017, **31**, 84–113.
137 V. Maltese, S. Cospito, A. Beneduci, B. C. De Simone, N. Russo, G. Chidichimo and R. A. J. Janssen, *Chem. – Eur. J.*, 2016, **22**, 10179–10186.
138 G. Chen, H. Sasabe, Y. Sasaki, H. Katagiri, X.-F. Wang, T. Sano, Z. Hong, Y. Yang and J. Kido, *Chem. Mater.*, 2014, **26**, 1356–1364.
139 T. Maeda, S. Mineta, H. Fujiwara, H. Nakao, S. Yagi and H. Nakazumi, *J. Mater. Chem. A*, 2013, **1**, 1303–1309.
140 B. M. Gridley, G. J. Moxey, W. Lewis, A. J. Blake and D. L. Kays, *Chem. – Eur. J.*, 2013, **19**, 11446–11453.
141 It should be noted that, while not mentioned in this review, there are some interesting examples of low-coordinate copper β-diketiminate complexes in catalysis. Please refer to Webster's recent Dalton Perspective (ref. 27).
142 M. Soleilhavoup and G. Bertrand, *Acc. Chem. Res.*, 2015, **48**, 256–266.
143 K. V. Bukhryakov, R. R. Schrock, A. H. Hoveyda, P. Müller and J. Becker, *Org. Lett.*, 2017, **19**, 2607–2609.
144 L. G. Perla, J. M. Kulenkampff, J. C. Fettinger and P. P. Power, *Organometallics*, 2018, **37**, 4048–4054.